HHS Public Access

Author manuscript

Cytometry A. Author manuscript; available in PMC 2016 May 06.

Published in final edited form as:

Cytometry A. 2015 October ; 87(10): 897–907. doi:10.1002/cyto.a.22683.

Novel Flow Cytometric Analysis of the Blood–Brain Barrier

Dionna W. Williams[1], **Lydia Tesfa**[2], and **Joan W. Berman**[1,2,*]

[1]Department of Pathology, Albert Einstein College of Medicine, Bronx, New York, 10461

[2]Department of Microbiology and Immunology, Albert Einstein College of Medicine, Bronx, New York, 10461

Abstract

The blood–brain barrier (BBB) is primarily comprised of brain microvascular endothelial cells (BMVEC) and astrocytes and serves as a physical and chemical barrier that separates the periphery from the brain. We describe a flow cytometric method using our in vitro model of the human BBB to characterize BMVEC surface junctional proteins critical for maintenance of barrier function, cell viability, and leukocyte adhesion. For this methodology, BMVEC are cocultured with astrocytes in a transwell tissue culture insert to establish the barrier, after which time the BBB are treated with specific agents, and the BMVEC collected for flow cytometric analyses. We use a standard and optimized method to recover the BMVEC from the coculture model that maintains junctional protein expression and cell viability. A novel leukocyte adhesion assay enables a quantitative analysis of peripheral blood mononuclear cell (PBMC) interactions with the BMVEC and can be used to assess the adhesion of many cell types to the BBB. Furthermore, this method enables the concomitant analysis of a large number of adhesion molecules and tight junction proteins on both the BMVEC and adherent PBMC under homeostatic and pathologic conditions. Flow cytometry is an extremely powerful tool, and this technique can also be applied to assess variables not performed in this study, including cell cycle progression, and calcium flux.

Key terms

adhesion molecule; tight junction protein; brain microvascular endothelium; leukocyte–endothelial cell interaction; adhesion; flow cytometry

---

The blood–brain barrier (BBB) consists of a complex network of cellular constituents that line the brain microvascular capillaries that separate the peripheral blood from the brain parenchyma. (1) Brain microvascular endothelial cells (BMVEC) are one of the major cellular components of the BBB. These cells have extensive tight junctions and adhesion molecules at interendothelial cell–cell junctions that facilitate maintenance of barrier integrity. Some of these molecules include zonula occludens-1, claudins, cadherins, occludin, junctional adhesion molecule-A (JAM-A), activated leukocyte cellular adhesion molecule (ALCAM), platelet/endothelial cell adhesion molecule (PECAM-1), the single-

*Correspondence to: Joan W. Berman; Department of Pathology, F727, Albert Einstein College of Medicine, 1300 Morris Park Ave. Bronx, NY, 10461, USA. joan.berman@einstein.yu.edu.

Additional Supporting Information may be found in the online version of this article.

chain type-1 glycoprotein CD99, intercellular adhesion molecule 1 (ICAM-1), and cellular prion protein (PrP^C). These proteins interact homo- and heterotypically to form dynamic structures that establish a tightly sealed endothelial cell layer. (2) They contribute to low paracellular permeability and high electrical resistance, prevent lateral diffusion, and maintain BMVEC polarity. (3–5) The adhesion molecules, adherens junctions, and tight junction proteins, which we collectively term junctional proteins, are highly responsive to stimuli and quickly undergo remodeling to ensure homeostasis. However, during many inflammatory and neurodegenerative disorders, including stroke (6), epilepsy (7), and multiple sclerosis (8), these junctional molecules become compromised, an insult to the BBB that contributes to central nervous system (CNS) dysfunction. In addition to their role in facilitating endothelial cell integrity, junctional molecules also promote leukocyte trafficking across the BBB into the CNS (9–11).

There has been much interest in developing in vitro models that reflect the well-organized and unique properties of the BBB that can be used to assess vascular dysfunction during pathogenesis, to characterize drug permeabilities, and to examine mechanisms that contribute to leukocyte diapedesis across the brain vasculature (12). Previous findings using in vitro BBB models have furthered our knowledge of barrier properties and the molecular mechanisms contributing to its function. However, a major limitation of many these systems is that they can be utilized only for the sole application for which they have been designed. A methodology with a large number of applications would enable a more complete understanding of the BBB, both during physiologic and pathologic processes.

In this study, we describe a novel flow cytometric method for the analysis of BMVEC after coculture with astrocytes in our in vitro BBB model. We optimized the use of a reagent that gently recovers the BMVEC from BBB cocultures that enabled the examination of endothelial adhesion molecule and tight junction protein surface expression, as well as quantification of leukocyte adhesion to the barrier. The studies performed here represent only a small number of the functional assays that can be used with this technique. While we introduce this new method by examining BMVEC proteins, the strength of this methodology is in its ability to be used in a wide variety of experimental settings and, due to the technical advances in flow cytometric techniques, enables concurrent analysis of many biological factors, including nucleic acids, proteins, and small molecules.

Materials and Methods

Materials

Human brain microvascular endothelial cells (BMVEC) were from Applied Cell Biology Research Institute (Kirkland, WA). Cortical astrocytes were obtained as part of an ongoing, approved research protocol at the Albert Einstein College of Medicine. Ficoll-Paque PLUS was from GE Healthcare (Uppsala, Sweden). Medium 199 (M199), L-glutamine, penicillin–streptomycin, newborn calf serum, phosphate-buffered saline (PBS), Dulbecco's modified eagle medium (DMEM), fetal bovine serum (FBS), and Hank's balanced salt solution (HBSS) were from Gibco (Grand Island, NY). Sodium bicarbonate, ascorbic acid, heparin sodium salt, endothelial cell growth supplement, ethylenediaminetetraacetic acid (EDTA), lidocaine hydrochloride monohydrate, and lipopolysaccharide (LPS) from *E. Coli* 055:B5

were from Sigma-Aldrich (Saint Louis, MO). HEPES was from Teknova (Hollister, CA). Bovine brain extract was from Clonetics/Lonza (Walkersville, MD). Human serum type AB was from Corning (Corning, NY). Gelatin and bovine serum albumin (BSA) were from Thermo Fisher Scientific (Walther, MA). Tissue culture inserts containing membranes with 3-μm pores, Annexin V PE Apoptosis Detection Kit, fluorochrome conjugated monoclonal antibodies specific for human PECAM-1 (clone WM59), CD99 (clone TU12), JAM-A (clone M.Ab F11), ICAM (clone HA58), CD45 (clone 2D1), CD14 (clone M5E2), CD3 (clone HIT3a), CD66b (clone G10F5), and respective isotype-matched negative controls were from BD Falcon (Franklin Lakes, NJ). Biotin-conjugated anti-human ALCAM (clone 105902) monoclonal antibody, its respective biotin-conjugated isotype-matched negative control, and vascular endothelial cell growth factor (VEGF) were obtained from R&D Systems (Minneapolis, MN). PE-coupled anti-human PrP^C monoclonal antibody (clone 4D5) and PE-conjugated streptavidin were obtained from eBiosciences (San Diego, CA). APC-coupled anti-human occludin rabbit polyclonal antibody and its respective negative control were obtained from Bioss (Woburn, MA). Paraformaldehyde aqueous solution was from Electron Microscopy Sciences (Hatfield, PA). Trypsin-EDTA (0.05%), TrypLE Express, and Accutase Cell Dissociation Reagent were obtained from Invitrogen (Grand Island, NY). Mini cell scrapers were from United BioSystems (Herndon, VA).

Experiment Overview

We developed a standardized flow cytometry-based method to evaluate dynamic changes in endothelial cell surface protein expression and leukocyte–endothelial cell interactions using an in vitro model of the human BBB. This standardized method provides a useful tool to study the effects of pharmacologic agents on the proteins of the endothelial vasculature comprising the BBB, as well as the functional consequences these perturbations may have on recruiting leukocytes to the brain. This methodology has applications for the study of neuroinflammation mediated by peripheral blood cell influx into the CNS parenchyma.

All experiments were performed with at least three replicates for each treatment group, three independent times (n =3). Isotype-matched negative controls and FMO controls were used for every detection antibody and in multicolor staining parameters, respectively, as appropriate. Unstained cells were also used as controls for all experiments in this study.

Biological Specimen Description

BMVEC were grown on cell culture dishes coated with 0.2% gelatin in supplemented M199 media (M199C) (containing M199, 0.05 M sodium bicarbonate, 0.03 μM HEPES, 0.8% L-glutamine, 1% penicillin–streptomycin, 50 mg/mL ascorbic acid, 25 mg/mL heparin sodium salt, 3 mg/mL endothelial cell growth supplement, 9 mg/mL bovine brain extract, 5% human serum-type AB, and 20% newborn calf serum) and used at passages 10–17 to establish the BBB model. Astrocytes were grown in supplemented DMEM media (containing DMEM, 10% FBS, and 1% penicillin–streptomycin) and used at passages 3–5 to establish the BBB model.

Peripheral blood was collected from deidentified donors according to established protocols at the Albert Einstein College of Medicine. The blood was diluted with an equal volume of

HBSS and peripheral blood mononuclear cells (PBMC) isolated within 1 h of blood draw by density gradient centrifugation using Ficoll-Paque PLUS. The PBMC were washed once with HBSS and resuspended in M199C.

In Vitro Model of the Human BBB

To establish in vitro model of the human BBB, astrocytes were resuspended at 5×10^5 cells/mL in M199C and 200 μL of cells seeded on the underside of tissue culture inserts as previously described (13–15). M199C was added continuously to the inserts at 10- to 15-min intervals for 4 h to allow for astrocyte adhesion to the membrane filter. The inserts were then turned right side up and placed in the wells of a 24-well plate containing M199C. BMVEC were then resuspended at 2×10^5 cells/mL in M199C and 200 μL of cells added to the upper side of gelatinized transwell inserts. After two days, the BMVEC-astrocyte cocultures were transferred to low serum M199C (M199C with 10% newborn calf serum and no human serum AB) for 24 h to reduce platelet-derived growth factor. After 3 days of coculture, the confluent BMVEC and astrocytes establish a tight barrier with a high transendothelial electrical resistance (TEER), impermeability to albumin and tritiated inulin, and expression of many markers consistent with the human BBB, as previously described (14,16). Thus, cocultures were used for all subsequent applications 3 days after they were established.

BMVEC Recovery Assay

To recover BMVEC from the BBB model, 200 μL of each dissociation agent was added to the apical side of the tissue culture insert and the cocultures incubated at 37 °C, 5% CO_2 until the endothelial cells appeared rounded and lifted from the transwell membrane upon visualization by light microscopy. Following incubation, 200 μL of M199C were added to the apical side of the coculture and the loosely bound BMVEC collected by pipetting and gentle scraping with a mini cell lifter. The recovered cells from each transwell were then transferred to an appropriate tube for fluorescent antibody labeling.

To confirm that our model could be used to assess the effects of selected agents on BBB endothelium, we treated the apical side of coculture transwells with LPS or VEGF (both at 10 ng/mL), or PBS vehicle control for 24 h. Each treatment condition was performed with four replicate cocultures. Following treatment, the apical side of the tissue culture insert was washed twice with 200 μL PBS prior to addition of the dissociation agents. The BMVEC were then recovered from the BBB model as described previously and illustrated in Figure 1A.

It is recommended to recover the BMVEC from no more than 8 transwells at a time. This is especially important when performing experiments when cells are to be collected from more than 24 BBB model transwell inserts. As the BMVEC lift from the coculture insert, the barrier becomes compromised permitting the media from the top of the transwell, and some BMVEC as well, to flow through. The staggered collection of the BMVEC from the coculture inserts permits adequate time to collect all of the cells while minimizing potential cell loss.

Leukocyte BBB Adhesion Assay

To assess leukocyte adhesion to the BBB, 5×10^5 PBMC were added to the top of each BBB coculture transwell for 1 h at 37 °C, 5% CO_2 as indicated in Figure 1B. The BBB model can remain untreated to examine adhesion under baseline conditions, or it can be pretreated with factors that increase endothelial cell adhesion proteins (e.g., 10 ng/mL LPS or PBS diluent pretreatment for 24 h) to assess the effects of selected agents on leukocyte adhesion. After incubation for 1 h, non-adherent PBMC were removed by gently washing the top of the transwell twice with 200 μL PBS. The PBMC that adhered to the BBB were then recovered along with the BMVEC using TrypLE as described previously.

Flow Cytometry

The collected BMVEC were washed once with cold FACS buffer (PBS supplemented with 1% BSA) and the cells stained with fluorochrome-coupled antibodies specific for PECAM-1, ALCAM, CD99, PrP^C, JAM-A, ICAM-1, and occludin, or with corresponding isotype-matched negative control antibodies in a volume of 100 μL in the dark, on ice for 30 min. FMO controls were not used for this portion of experiments as only single staining was performed. All antibodies were titered to determine optimal concentrations for staining. Following staining, the cells were washed with FACS buffer and then fixed with 250 μL 2% paraformaldehyde. The fixed cells were filtered using BD FACS tubes with cell strainer caps with 35-μm pores and transferred to a U-bottom 96-well plate. The 96-well plate was covered with a multiwell sealing film and stored at 4 °C, wrapped in foil, up to 1 week prior to flow cytometric analysis.

For cell viability analyses, Annexin V and 7AAD staining were performed according to the manufacturer's protocol. Briefly, BMVEC collected from transwells were washed twice with cold PBS, resuspended in the provided binding buffer and stained in the dark for 15 min at room temperature with PE Annexin V and 7-AAD. Heating BMVEC at 55 °C for 10 min and vigorous scraping of the cells served as positive controls for apoptosis. The cells were analyzed by flow cytometry within 30 min of staining.

For the leukocyte BBB adhesion assay, the collected PBMC and BMVEC were immunostained for CD45 FITC, CD14 APC-Cy7, CD3 PE, and ICAM APC or isotype-matched control antibodies. FMO controls were prepared using an aliquot of the PBMC. Following staining, the cells were washed, fixed, filtered, transferred to a 96-well plate, and stored as described previously.

Instrument Details

A BD FACS Canto II flow cytometer with two lasers (485 and 633 nm) was used for this study. Cytometer setup and tracking beads were used to run daily measurements. The instrument was calibrated weekly using BD Calibrite Beads. The instrument configuration consisted of photomultiplier tubes arranged in one octagon and one trigon (a 4–2 optical configuration). The BD high-throughput sampler (HTS) was used in standard throughput sampling mode with the 96-well plates to enable automated enumeration of the acquired events. The fluidic instrument settings for acquisition utilizing the BD HTS are as follows:

175 μL sample volume, sample rate 3 μL/sec, mixing volume 100 μL, mixing speed 200 μL/sec for a total of two mixes, and a probe wash volume of 400 μL.

Data Analysis

The samples were acquired as list-mode files (FCS3.0 format) using BD FACSDiva software (v 6.1.3) using hardware compensation at the time of acquisition. Single-color controls were prepared using the same conjugated antibodies used in the study on the appropriate target cells. The compensation matrix is described in Table 1. Data were visualized on linear scale for forward and side scatter, and on logarithmic scale for fluorescence channels.

The samples were analyzed using FlowJo software (TreeS-tar v 10.0.6, Ashland, OR). For experiments where only BMVEC were acquired, a first gate consisted of FSC height versus area parameters to identify "singlets," excluding FSC-Area^{high} doublets, followed by SSC-Area versus FSC-Area to identify "BMVEC" (Fig. 3A–3B). The BMVEC were then characterized by their fluorescence intensities. For leukocyte adhesion experiments, an SSC-Area versus FSC-Area gate was used to subdivide the "PBMC" (SSC-Area^{low}, FSC-Area^{low}) from the "BMVEC" (SSC-Area^{high}, FSC-Area^{high}) (Fig. 5). The BMVEC were then analyzed according to APC fluorescence intensity. The PBMC were further gated to identify the "Monocytes" (CD45^{+}CD14^{+}) and the "T cells" (CD45^{+}CD3^{+}) (Fig. 5). The total events obtained within the monocyte and T-cell gates were then used to quantify the numbers of each leukocyte population that adhered to the BMVEC comprising BBB.

Statistical Analysis

Statistical analyses were performed using Prism 6.0 software (GraphPad Software, Inc., San Diego, CA). Two-tailed paired *t*-test was used to determine statistical significance ($P \leq 0.05$). A single asterisk (*) indicates $P \leq 0.05$ and double asterisks (**) indicate $P \leq 0.01$.

Results

TrypLE Is the Preferred Agent for the Recovery of BMVEC from BBB

Five reagents were used during initial studies to determine the optimal conditions for BMVEC recovery from our in vitro model of the human BBB. The selected agents included trypsin, 0.5 mM EDTA, accutase, 0.5% lidocaine, and TrypLE, that have distinct mechanisms mediating dissociation of adherent cells. Trypsin, a frequently used cell culture dissociation agent, consists of a mixture of proteases that detach adherent cells by cleaving lysine or arginine residues within cell surface proteins. While extremely efficient in recovering adherent cells, the extent of amino acid cleavage mediated by trypsin often limits its use in subsequent cell surface protein applications, including flow cytometry (17). EDTA is a compound that chelates divalent cations. As cell adhesion is a Ca^{+2}-dependent process, agents that promote its sequestration, such as EDTA, can be used to facilitate cell lifting. Accutase is an enzyme with collagenase and protease activity commonly used as a substitute for trypsin when the gentle detachment of adherent cells is needed, particularly for flow cytometric applications (18). Lidocaine is a local anesthetic that can also be used to harvest adherent cells. Lidocaine facilitates dissociation by reversibly inhibiting cell adhesion and spreading (19,20). However, caution must be taken with lidocaine, as it is toxic to some

cells, including neurons (21,22). The final reagent was TrypLE, a trypsin-like substitute comprised of a proprietary recombinant protease and EDTA. Try-pLE is a comparable, but gentler alternative to trypsin that is becoming widely used as it maintains surface protein expression (23–25).

Our objective was to identify the dissociation agent that (1) recovered the majority of the BMVEC from the BBB model, (2) required the shortest amount of time, and (3) resulted in minimal cell death and proteolysis-mediated epitope loss. To accomplish this goal, we added 200 μL of each dissociation agent to the top of the BBB transwell and incubated the cocultures at 37 °C, 5% CO_2 until the endothelial cells lifted from the filter. The cocultures were examined by light microscopy at 5 min intervals to determine the duration of time necessary for the BMVEC to become rounded and in suspension. The viability of the BMVEC recovered using each dissociation agent was determined by trypan blue exclusion. The results of three independent experiments are listed in Table 2. Nearly, 100% of the BMVEC were recovered from the transwells using each dissociation agent upon inspection of the coculture filter insert by light microscopy (data not shown). None of the dissociation agents were toxic to the BMVEC, and there were no significant differences in the viabilities of the recovered cells (Table 2). However, there were differences in the amount of time it took to recover the BMVEC. As expected, trypsin had the shortest dissociation time of 5.3 ±2.5 min. With a time of 13.3 ±1.5 min, TrypLE was the second fastest dissociation agent. In contrast, accutase, lidocaine, and EDTA required much longer times to dissociate the BMVEC from the BBB model (Table 2).

We next confirmed the viability of the recovered BMVEC with Annexin V and 7AAD. BMVEC that were recovered by vigorous scraping (without the use of any dissociation agent), or following heating at 55 °C for 10 min, were used as positive controls for apoptosis. Additionally, we examined cell surface expression of JAM-A, a tight junction molecule highly expressed in BMVEC that is critical for the maintenance of BBB integrity and for facilitating leukocyte transmigration across the vasculature, as an indicator of cell surface protein degradation. The recovered BMVEC were viable following recovery with both trypsin and TrypLE, as only ~7% of the cells were positive for Annexin V and 7AAD (Fig. 2A). Similar viabilities were observed following recovery with accutase, lidocaine, and EDTA (data not shown). In contrast, heating and vigorous scraping of the cells caused substantial cell death (Fig. 2A).

JAM-A was present on the BMVEC cell surface following recovery from the BBB model (Fig. 2B). However, the mean fluorescence intensity (MFI) of JAM-A was 600 units higher following TrypLE dissociation as compared to recovery with trypsin (Fig. 2B). The expression of JAM-A following recovery with TrypLE was similar to that obtained upon dissociation with accutase, lidocaine, and EDTA (data not shown). PECAM-1 was also reduced on the BMVEC cell surface upon recovery with trypsin, as compared to the other cell dissociation reagents (data not shown). This is in agreement with the work of others, as PECAM-1 is known to be sensitive to trypsin cleavage (26). TrypLE was used exclusively for the remainder of experiments in this study to recover quickly the BMVEC while minimizing the potential for the degradation of surface protein epitopes. While these experiments were optimized for our proteins of interest, it is important to determine the

effect of TrypLE on cleavage of additional proteins to ensure optimal results in future experiments.

Dynamic Changes in Adhesion Molecule and Tight Junction Proteins of the BBB

The BMVEC comprising the BBB are highly specialized, nonfenestrated endothelial cells with extensive tight junction proteins and adhesion molecules. These junctional proteins interact with opposing BMVEC, facilitating cell–cell adhesion, and restricting para- and transcellular passage across the BBB. Therefore, junctional proteins are essential for maintaining barrier function. Our transwell model of the human BBB enables the study of these molecules on BMVEC upon coculture with astrocytes, which is critical for maintaining the integrity of these molecules in an in vitro setting. The flow cytometry-based method described here allows for multiparametric analysis of a large number of junctional proteins, as many flow cytometers can be configured to detect simultaneously up to 14 colors.

We first assessed the expression of BMVEC junctional proteins under baseline conditions. BMVEC were recovered from the BBB model and PECAM-1, ALCAM, CD99, and PrP^C measured by flow cytometry using the method described previously. Following doublet discrimination (Fig. 3A), BMVEC were identified by light scatter characteristics (Fig. 3B). In agreement with previous findings, PECAM-1 (Fig. 3C), ALCAM (Fig. 3D), CD99 (Fig. 3E), and PrP^C (Fig. 3F) were highly expressed on the BMVEC recovered from our BBB model. The expression of these proteins was highly reproducible upon recovering the BMVEC from the BBB in six independent experiments (Fig. 3G).

We next characterized BMVEC junctional proteins following treatment with mediators known to alter endothelial cell signaling and subsequent protein expression to confirm that our analysis quantifies changes in junctional protein expression in BBB endothelium. The BBB model was treated with 10 ng/mL LPS or VEGF, or PBS vehicle control, for 24 h, after which time the BMVEC were recovered with TrypLE and analyzed by flow cytometry. While present on the cell surface under baseline conditions, ICAM was significantly increased on BMVEC following treatment with LPS (Fig. 4A–4B). We observed similar findings upon treating with 1 and 100 ng/mL LPS (data not shown). LPS promotes endothelial cell activation and is known to upregulate many adhesion molecules to facilitate leukocyte recruitment and subsequent diapedesis. We also examined the tight junction protein occludin and determined that, as expected, it was expressed by BMVEC (Fig. 4C). VEGF, an angiogenic factor that promotes endothelial tube formation, significantly reduced occludin after treatment with 10 ng/mL of the growth factor for 24 h (Fig. 4C–4D), which is in agreement with the work of others (27). Treatment with VEGF at 1 ng/mL also caused a decrease in occludin, while treatment at 0.1 ng/mL did not alter the tight junction protein (data not shown). These findings indicate that the BMVEC recovered from our BBB model express junctional molecules and are responsive to stimuli. These data attest to the use of this flow cytometry based technique to assess dynamic changes in the surface expression of proteins that mediate BBB permeability and integrity.

Leukocyte Adhesion to the BBB

Leukocyte recruitment to the BBB is critical for immune surveillance of the brain (28,29). Importantly, cellular influx into the CNS also occurs during many neuroinflammatory and neurodegenerative diseases and often contributes to the pathogenesis of these disorders. Adhesion to the BBB is the first step in a well-ordered, multistep process that results in leukocyte entry into the brain. Adhesion is facilitated by homo- and heterophilic interactions between the leukocytes and the BMVEC. Leukocyte adhesion assays have been widely used to evaluate the functional consequences of perturbations in endothelial cell junctional proteins mediated by various treatment conditions in vitro and in vivo during pathologic states. However, many of these studies were performed using endothelial cells from the peripheral vasculature, which are less complex than the BMVEC, and may not be suitable for the study of mechanisms specific to CNS leukocyte recruitment. We now describe a novel flow cytometric assay to evaluate cellular adhesion in a model of the human brain vasculature.

A schematic description of the leukocyte adhesion methodology is depicted in Figure 1B. Our in vitro human BBB model can be used to assess leukocyte adhesion following pre-treatment of BBB endothelium with an agent of interest, or when the barrier remains untreated to evaluate basal adhesion. PBMC can then be added to the upper portion of the BBB transwell for 1 h. The adherent leukocytes are then recovered along with the BMVEC from which they were interacting using TrypLE, and the cells analyzed by flow cytometry. This adhesion assay enables the study of changes in BMVEC junctional proteins with the simultaneous analysis of PBMC subsets that adhered to the BBB.

We evaluated leukocyte adhesion following treatment with a vehicle control (Fig. 5A) or LPS (Fig. 5B), a known inducer of endothelial cell adhesion molecules resulting in an increased leukocyte–endothelial cell adhesion (30,31). Scatter characteristics were used to gate on the BMVEC, followed by the analysis of fluorescence intensities for ICAM-1. We first confirmed that LPS increased the expression of ICAM-1 on the BMVEC cell surface (BMVEC in Fig. 5B compared to Fig. 5A). This assay may also be used to examine other adhesion molecules in addition to ICAM-1 that may be altered upon leukocyte adhesion to the BBB. Next, we analyzed the adherent PBMC population using the pan-leukocyte marker CD45, along with monocyte and T-cell-specific markers CD14 and CD3, respectively. Rectangle gates were made on $CD45^+CD14^+$ and $CD45^+CD3^+$ cells for the vehicle-treated cocultures and applied to the LPS-treated samples. The events acquired within those gates were enumerated to quantify the number of cells that adhered to the BBB.

Approximately, 20,000 $CD14^+$ (Fig. 5C) and $CD3^+$ (Fig. 5D) cells adhered to each well of the BBB insert under baseline conditions. The number of monocytes and T cells that adhered to the BBB significantly increased upon treatment with LPS (Fig. 5C–5D). The same analyses were performed gating on $CD45^+CD66b^+$ cells within the PBMC to quantify neutrophil adhesion. Similar to the other leukocyte subsets, LPS also significantly increased neutrophil adhesion to the BBB (data not shown). This flow cytometric leukocyte BBB adhesion assay is very sensitive and highly reproducible, with variations in the number of adherent PBMC being <400 cells among triplicate coculture inserts for each treatment group. The quantification of the exact number of adherent cells provides a unique advantage

of this flow cytometric technique that is difficult to obtain with other assays, such as microscopic or fluorescence multiwell plate methods. It is important to note that this assay may underrepresent the number of adherent cells to the BBB, as cell migration may have occurred across the barrier. In an attempt to minimize this possibility, we performed the adhesion assay for 1 h. It is recommended to optimize the duration of the leukocyte adhesion assay for each cell population of interest.

Discussion

The flow cytometry-based method described here allows for the examination of endothelial junctional proteins that facilitate barrier impermeability and for the quantitative assessment of leukocyte adhesion to the BBB. This technique is a novel application of our well-established model of the human BBB. The BMVEC/astrocyte coculture system has many properties of the BBB and provides an appropriate in vitro model of brain microvasculature. We confirmed that the BMVEC from this transwell model had extensive adhesion molecule and tight junction proteins and that the cells were viable following recovery using TrypLE. We demonstrated that the BMVEC were responsive to LPS and VEGF treatment as an example of one of the applications of this method. Flow cytometry is a powerful tool that enables the analysis of many sophisticated processes. In addition to cell surface protein and cell viability analyses, this technique also affords the possibility to examine cell cycle progression, signal transduction, calcium flux, RNA expression, and cytokine and reactive oxygen species production.

Our flow cytometric method may also be used for other applications, including assessing drug transport. This is an important area of research as over 98% of small and large molecule drugs fail to penetrate the BBB (32). We have consistently used our BBB model to assess barrier permeability, by exclusion of Evans blue conjugated albumin and tritiated inulin, and by TEER. In addition to these permeability methods, we can now use the flow cytometric assay to identify mechanisms contributing to drug transport across the BBB, including adenosine triphosphate cassette expression and function (33–35).

Our leukocyte adhesion assay also has many applications. While we examined the total population of CD14 monocytes and CD3 T cells in this study, there are subsets within these leukocyte classifications, and the adhesion of these subpopulations to the BBB is implicated in many disorders. This assay could be used to evaluate the adhesion of $CD14^{+}CD16^{-}$, $CD14^{+}CD16^{+}$, and $CD14^{low}CD16^{+}$ monocytes to the BBB both under baseline conditions, and following treatment with factors that model CNS pathologic states. Additionally, the adhesion assay can also be performed with a purified population of leukocytes, such as $CD3^{+}$ cells, to determine the relative adhesion of the T helper subsets, including Th1, Th2, Th17, and regulatory T cells, simultaneously. This provides an easier, less time intensive method than other leukocyte adhesion assays, such as fluorescence assays with microplate readers or microscopy.

The collective analyses of both adherent cells and BMVEC can be applied to many elegant experimental settings. For example, platelets and monocytes can be added concurrently to examine the effect of select conditions on platelet/monocyte aggregates at the BBB, and the

resultant effects on BMVEC, as this is important for the development of CNS inflammation (36,37). Additionally, the adhesion assay need not only be performed with leukocytes, but can also be used to evaluate adhesion of any cell of interest to the BBB. One such example is the evaluation of the adhesion of breast cancer cell lines to the BBB prior to and following siRNA knockdown of a putative target that facilitates invasion. This has many clinical ramifications, as adhesion to the vasculature is the first step in metastasis (38,39). This method has applications for neurotropic pathogens as well, such as HIV, *Cryptococcus neoformans*, and *Plasmodium,* as all of these infectious agents are associated with increased leukocyte influx into the CNS and BBB compromise that result in disease (40–45).

There are limitations to our methodology, including the fact that our model of the human BBB lacks pericytes, an important cell type that regulates vascular tone and contributes to barrier functions (46–48). Additionally, our transwell model of the BBB is cultured under static conditions and is unable to capture its fluid nature as blood continuously passes through the cerebral microvessels. Despite these limitations, our findings demonstrate that this method reliably evaluates BBB junctional proteins, BMVEC viability following various treatment conditions and provides a quantitative analysis of leukocyte adhesion. This flow cytometric analysis of the BBB is not restricted to the assays performed herein but has many applications to diverse scientific areas as well.

Acknowledgments

Grant sponsor: Mount Sinai Institute for NeuroAIDS Disparities, Grant number: R25 MH080663 (DWW), T32AI070117 (DWW).

Grant sponsor: UNCF/Merck Graduate Science Dissertation Fellowship (DWW), Grant number: MH075679 (JWB), MH090958 (JWB), DA025567 (JWB)

Grant sponsor: Flow Cytometry Core Facility, Grant number: P30CA013330 (LT)

Grant sponsor: Center for AIDS Research at the Albert Einstein College of Medicine and Montefiore Medical Center, Grant number: AI051519

We would like to thank Drs. Eliseo A. Eugenin, Tina Calderon, Peter. J. Gaskill, Jackie Coley, and Brad Poulos, as well as Lillie Lopez, Bezawit Megra, Mike Veenstra, and Matias Jaureguiberry, for valuable contributions to this project.

Literature Cited

1. Obermeier B, Daneman R, Ransohoff RM. Development, maintenance and disruption of the blood-brain barrier. Nat Med. 2013; 19:1584–1596. [PubMed: 24309662]
2. Ballabh P, Braun A, Nedergaard M. The blood-brain barrier: An overview: Structure, regulation, and clinical implications. Neurobiol Dis. 2004; 16:1–13. [PubMed: 15207256]
3. Balda MS, Matter K. Tight junctions and the regulation of gene expression. Biochimica Et Biophysica Acta (BBA) - Biomembranes. 2009; 1788:761–767. [PubMed: 19121284]
4. Bazzoni G. Pathobiology of junctional adhesion molecules. Antioxid Redox Signal. 2011; 15:1221–1234. [PubMed: 21254840]
5. Lampugnani MG, Dejana E. Adherens junctions in endothelial cells regulate vessel maintenance and angiogenesis. Thromb Res. 2007; 120:S1–S6. [PubMed: 18023702]
6. Liu J, Jin X, Liu KJ, Liu W. Matrix metalloproteinase-2-mediated occludin degradation and caveolin-1-mediated claudin-5 redistribution contribute to blood–brain barrier damage in early ischemic stroke stage. J Neurosci. 2012; 32:3044–3057. [PubMed: 22378877]

7. van Vliet EA, Aronica E, Gorter JA. Role of blood–brain barrier in temporal lobe epilepsy and pharmacoresistance. Neuroscience. 2014; 277:455–473. [PubMed: 25080160]
8. Alvarez JI, Cayrol R, Prat A. Disruption of central nervous system barriers in multiple sclerosis. Biochim Biophys Acta. 2011; 1812:252–264. [PubMed: 20619340]
9. Muller WA. Getting leukocytes to the site of inflammation. Vet Pathol. 2013; 50:7–22. [PubMed: 23345459]
10. Takeshita Y, Ransohoff RM. Inflammatory cell trafficking across the blood–brain barrier: Chemokine regulation and in vitro models. Immunol Rev. 2012; 248:228–239. [PubMed: 22725965]
11. Williams DW, Calderon TM, Lopez L, Carvallo-Torres L, Gaskill PJ, Eugenin EA, Morgello S, Berman JW. Mechanisms of HIV entry into the CNS: Increased sensitivity of HIV infected cd14+cd16+ monocytes to ccl2 and key roles of ccr2, JAM-a, and ALCAM in diapedesis. PLoS ONE. 2013; 8:e69270. [PubMed: 23922698]
12. He Y, Yao Y, Tsirka SE, Cao Y. Cell-culture models of the blood–brain barrier. Stroke. 2014; 45:2514–2526. [PubMed: 24938839]
13. Hurwitz AA, Berman JW, Rashbaum WK, Lyman WD. Human fetal astrocytes induce the expression of blood-brain barrier specific proteins by autologous endothelial cells. Brain Res. 1993; 625:238–243. [PubMed: 7903899]
14. Eugenin EA, Berman JW. Chemokine-dependent mechanisms of leukocyte trafficking across a model of the blood-brain barrier. Methods. 2003; 29:351–361. [PubMed: 12725802]
15. Eugenin EA, Osiecki K, Lopez L, Goldstein H, Calderon TM, Berman JW. CCL2/monocyte chemoattractant protein-1 mediates enhanced transmigration of human immunodeficiency virus (HIV)-infected leukocytes across the blood-brain barrier: A potential mechanism of HIV-CNS invasion and NeuroAIDS. J Neurosci. 2006; 26:1098–1106. [PubMed: 16436595]
16. Weiss JM, Downie SA, Lyman WD, Berman JW. Astrocyte-derived monocyte-chemoattractant protein-1 directs the transmigration of leukocytes across a model of the human blood-brain barrier. J Immunol. 1998; 161:6896–6903. [PubMed: 9862722]
17. Gray DHD, Chidgey AP, Boyd RL. Analysis of thymic stromal cell populations using flow cytometry. J Immunol Methods. 2002; 260:15–28. [PubMed: 11792372]
18. Yuan SH, Martin J, Elia J, Flippin J, Paramban RI, Hefferan MP, Vidal JG, Mu Y, Killian RL, Israel MA, et al. Cell-surface marker signatures for the isolation of neural stem cells, glia and neurons derived from human pluripotent stem cells. PLoS ONE. 2011; 6:e17540. [PubMed: 21407814]
19. Rabinovitch M, Destefano MJ. Macrophage spreading in vitro: III. The effect of metabolic inhibitors, anesthetics and other drugs on spreading induced by subtilisin. Exp Cell Res. 1974; 88:153–162. [PubMed: 4371417]
20. Rabinovitch M, DeStefano MJ. Use of the local anesthetic lidocaine for cell harvesting and subcultivation. In Vitro. 1975; 11:379–381. [PubMed: 1201854]
21. Perez-Castro R, Patel S, Garavito-Aguilar ZV, Rosenberg A, Recio-Pinto E, Zhang J, Blanck TJJ, Xu F. Cytotoxicity of local anesthetics in human neuronal cells. Anesth Analg. 2009; 108:997–1007.10.1213/ane.0b013e31819385e1 [PubMed: 19224816]
22. Yu HZ, Li YH, Wang RX, Zhou X, Yu MM, Ge Y, Zhao J, Fan TJ. Cytotoxicity of lidocaine to human corneal endothelial cells in vitro. Basic Clin Pharmacol Toxicol. 2014; 114:352–359. [PubMed: 24373304]
23. Manira M, Anuar KK, Seet WT, Irfan AWA, Ng MH, Chua KH, Heikal MYM, Aminuddin BS, Ruszymah BHI. Comparison of the effects between animal-derived trypsin and recombinant trypsin on human skin cells proliferation, gene and protein expression. Cell Tissue Bank. 2014; 15:41–49. [PubMed: 23456438]
24. Aghayan, HR.; Goodarzi, P.; Arjmand, B. Methods in Molecular Biology. New York: Humana Press; 2014. GMP-Compliant Human Adipose Tissue-Derived Mesenchymal Stem Cells for Cellular Therapy; p. 1-15.
25. Bradford, J.; Clarke, S. Panel Development for Multicolor Flow-Cytometry Testing of Proliferation and Immunophenotype in hMSCs. In: Vemuri, M.; Chase, LG.; Rao, MS., editors. Mesenchymal

Stem Cell Assays and Applications. Vol. 698, Methods in Molecular Biology. New York: Humana Press; 2011. p. 367-385.

26. Marelli-Berg FM, Peek E, Lidington EA, Stauss HJ, Lechler RI. Isolation of endothelial cells from murine tissue. J Immunol Methods. 2000; 244:205–215. [PubMed: 11033033]
27. Argaw AT, Gurfein BT, Zhang Y, Zameer A, John GR. VEGF-mediated disruption of endothelial CLN-5 promotes blood-brain barrier breakdown. Proc Natl Acad Sci USA. 2009; 106:1977–1982. [PubMed: 19174516]
28. Kleine TO. Cellular immune surveillance of central nervous system bypasses blood–brain barrier and blood–cerebrospinal–fluid barrier: Revealed with the new marburg cerebrospinal–fluid model in healthy humans. Cytometry A. 2015; 87A:227–243. [PubMed: 25641944]
29. Kleine TO, Benes L. Immune surveillance of the human central nervous system (CNS): Different migration pathways of immune cells through the blood-brain barrier and blood-cerebrospinal fluid barrier in healthy persons. Cytometry A. 2006; 69A:147–151. [PubMed: 16479603]
30. Myers CL, Wertheimer SJ, Schembri-King J, Parks T, Wallace RW. Induction of ICAM-1 by TNF-alpha, IL-1 beta, and LPS in human endothelial cells after downregulation of PKC. Am J Physiol. 1992; 263:C767–C772. [PubMed: 1357985]
31. Sawa Y, Ueki T, Hata M, Iwasawa K, Tsuruga E, Kojima H, Ishikawa H, Yoshida S. LPS-induced IL-6, IL-8, VCAM-1, and ICAM-1 expression in human lymphatic endothelium. J Histochem Cytochem. 2008; 56:97–109. [PubMed: 17938282]
32. Pardridge WM. Blood–brain barrier delivery. Drug Discov Today. 2007; 12:54–61. [PubMed: 17198973]
33. García-Escarp M, Martínez-Muñoz V, Sales-Pardo I, Barquinero J, Domingo JC, Marin P, Petriz J. Flow cytometry–based approach to ABCG2 function suggests that the transporter differentially handles the influx and efflux of drugs. Cytometry A. 2004; 62A:129–138. [PubMed: 15517563]
34. Kooij G, van Horssen J, Bandaru VVR, Haughey NJ, De Vries HE. The role of ATP-binding cassette transporters in neuro-inflammation: Relevance for bioactive lipids. Front Pharmacol. 2012; 3
35. Dean M, Hamon Y, Chimini G. The human ATP-binding cassette (ABC) transporter superfamily. J Lipid Res. 2001; 42:1007–1017. [PubMed: 11441126]
36. Singh MV, Davidson DC, Jackson JW, Singh VB, Silva J, Ramirez SH, Maggirwar SB. Characterization of platelet–monocyte complexes in HIV-1–infected individuals: Possible role in HIV-associated neuroinflammation. J Immunol. 2014; 192:4674–4684. [PubMed: 24729609]
37. Mazereeuw G, Herrmann N, Bennett SA, Swardfager W, Xu H, Valenzuela N, Fai S, Lanctôt KL. Platelet activating factors in depression and coronary artery disease: A potential biomarker related to inflammatory mechanisms and neurodegeneration. Neurosci Biobehav Rev. 2013; 37:1611–1621. [PubMed: 23800745]
38. Seoane J, De Mattos-Arruda L. Brain metastasis: New opportunities to tackle therapeutic resistance. Mol Oncol. 2014; 8:1120–1131. [PubMed: 24953014]
39. Niikura N, Saji S, Tokuda Y, Iwata H. Brain metastases in breast cancer. Jpn J Clin Oncol. 2014
40. Freeman BD, Machado FS, Tanowitz HB, Desruisseaux MS. Endothelin-1 and its role in the pathogenesis of infectious diseases. Life Sci. 2014
41. Shikani HJ, Freeman BD, Lisanti MP, Weiss LM, Tanowitz HB, Desruisseaux MS. Cerebral malaria: We have come a long way. Am J Pathol. 2012; 181:1484–1492. [PubMed: 23021981]
42. Valcour V, Chalermchai T, Sailasuta N, Marovich M, Lerdlum S, Suttichom D, Suwanwela NC, Jagodzinski L, Michael N, Spudich S, et al. Central nervous system viral invasion and inflammation during acute HIV infection. J Infect Dis. 2012; 206:275–282. [PubMed: 22551810]
43. Spudich S, González-Scarano F. HIV-1-related central nervous system disease: Current issues in pathogenesis, diagnosis, and treatment. Cold Spring Harb Perspect Med. 2012; 2
44. Liu TB, Kim JC, Wang Y, Toffaletti DL, Eugenin E, Perfect JR, Kim KJ, Xue C. Brain inositol is a novel stimulator for promoting cryptococcus penetration of the blood-brain barrier. PLoS Pathogens. 2013; 9:e1003247. [PubMed: 23592982]
45. Kim JC, Crary B, Chang YC, Kwon-Chung KJ, Kim KJ. Cryptococcus neoformans activates RhoGTPase proteins followed by protein kinase C, focal adhesion kinase, and ezrin to promote

traversal across the Blood-brain barrier. J Biol Chem. 2012; 287:36147–36157. [PubMed: 22898813]

46. Wilhelm I, Fazakas C, Krizbai IA. In vitro models of the blood-brain barrier. Acta Neurobiol Exp (Wars). 2011; 71:113–128. [PubMed: 21499332]
47. Nakagawa S, Deli M, Nakao S, Honda M, Hayashi K, Nakaoke R, Kataoka Y, Niwa M. Pericytes from brain microvessels strengthen the barrier integrity in primary cultures of rat brain endothelial cells. Cell Mol Neurobiol. 2007; 27:687–694. [PubMed: 17823866]
48. Dohgu S, Takata F, Yamauchi A, Nakagawa S, Egawa T, Naito M, Tsuruo T, Sawada Y, Niwa M, Kataoka Y. Brain pericytes contribute to the induction and up-regulation of blood–brain barrier functions through transforming growth factor-β production. Brain Res. 2005; 1038:208–215. [PubMed: 15757636]

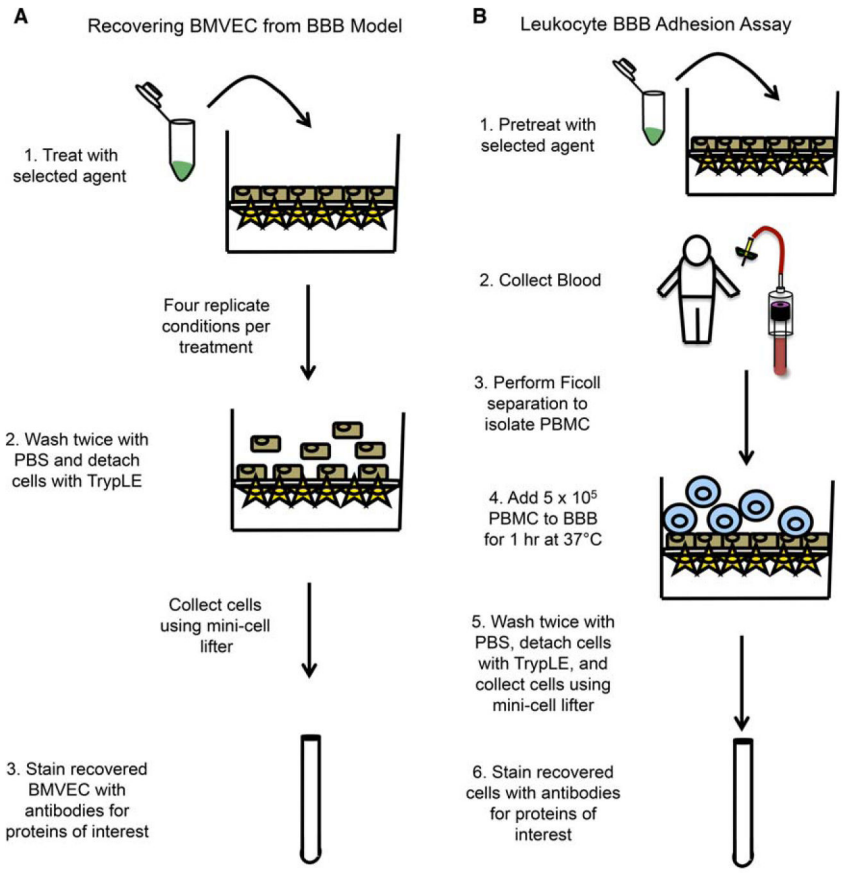

Figure 1.

Schematic representation of BMVEC recovery and leukocyte adhesion assays. The transwell model of the human BBB comprised of BMVEC and astrocytes cocultured on filters with 3-μm pores is established 3 days prior to the commencement of the experiment. (A) The apical side of the BBB transwell may then be treated with the selected agent of interest in four replicate conditions for the desired period of time. Following treatment, the BBB is rinsed twice with PBS, the supernatant discarded, TrypLE added, and the cocultures incubated for 13 min at 37 °C, 5% CO_2. The BMVEC are collected by pipetting and gentle scraping with a mini cell lifter and the cells transferred to an appropriate tube for FACS staining. (B) The BBB model is treated for the desired period of time prior to beginning the adhesion assay. PBMC are isolated from blood by density centrifugation with Ficoll-Paque PLUS and the cells (5×10^5) added to the transwell insert for 1 h at 37 °C, 5% CO_2. Following incubation, the nonadherent cells are removed by gently washing with PBS twice. The adherent PBMC are collected along with the BMVEC to which they were attached using TrypLE and gentle scraping with the mini cell lifter. The cells are then stained with antibodies for the proteins of interest. [Color figure can be viewed in the online issue, which is available at wileyonlinelibrary.com.]

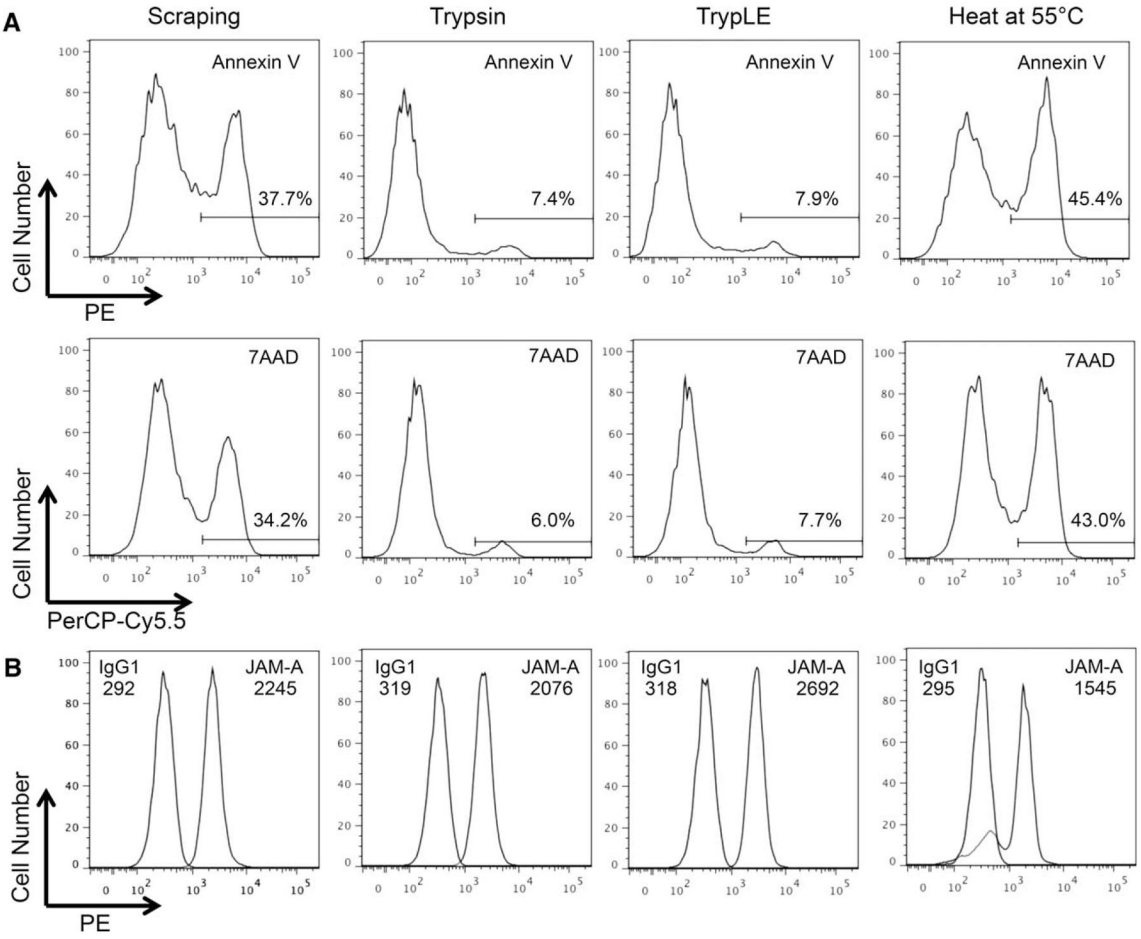

Figure 2.

Recovered BMVEC from BBB Model are viable and express JAM-A. BMVEC were collected from the BBB model following treatment with Trypsin, TrypLE, heating at 55 °C for 10 min, or by vigorous scraping in three individual experiments. (A) Cell viability was assessed with Annexin V and 7AAD. Representative histograms demonstrate the fluorescent signal for each of the indicated stains. A gate was made on the positive peak to enumerate the frequency of nonviable cells. (B) Representative histograms demonstrate the PE signal for JAM-A (open peak), its isotype-matched negative control (filled peak), and their respective mean fluorescence intensities (MFI).

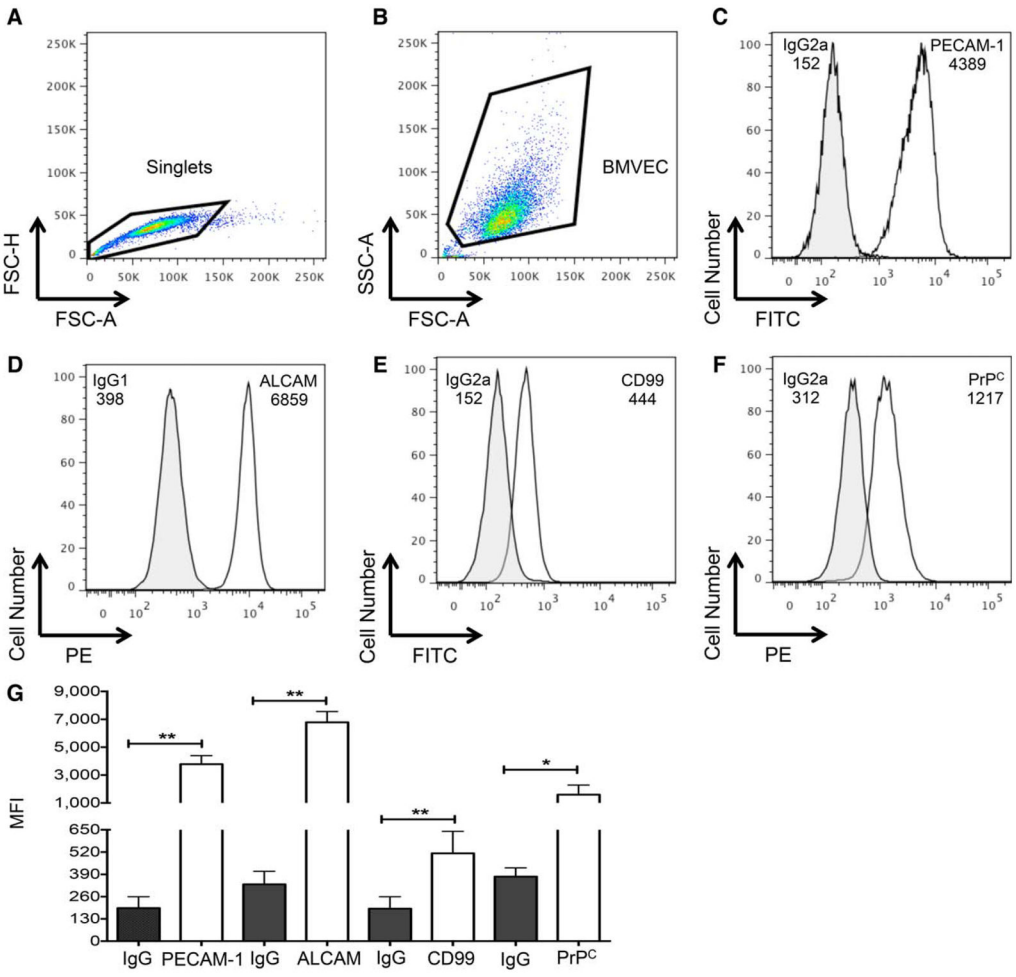

Figure 3.

BMVEC recovered from BBB model have extensive junctional proteins. BMVEC were collected from the BBB model using Try-pLE and junctional proteins examined by flow cytometry. (A) FSC-H and FSC-A were used for the identification of singlets (indicated within the gated population) and doublet discrimination. (B) The single cells were then examined by SSC-A and FSC-A to develop the BMVEC gate. FITC or PE fluorescent signal was used to examine (C) PECAM-1, (D) ALCAM, (E) CD99, (D) PrP^C and the respective isotype matched negative controls in one representative experiment. The MFI is denoted. (G) The MFI of PECAM-1, ALCAM, CD99, and PrP^C (open bars) or their respective isotype-matched negative controls (closed bars) were analyzed in six independent experiments. Data are represented as mean ±standard deviation. Significance was determined by a two-tailed paired *t*-test. **P* <0.05. ***P* <0.01. [Color figure can be viewed in the online issue, which is available at wileyonlinelibrary.com.]

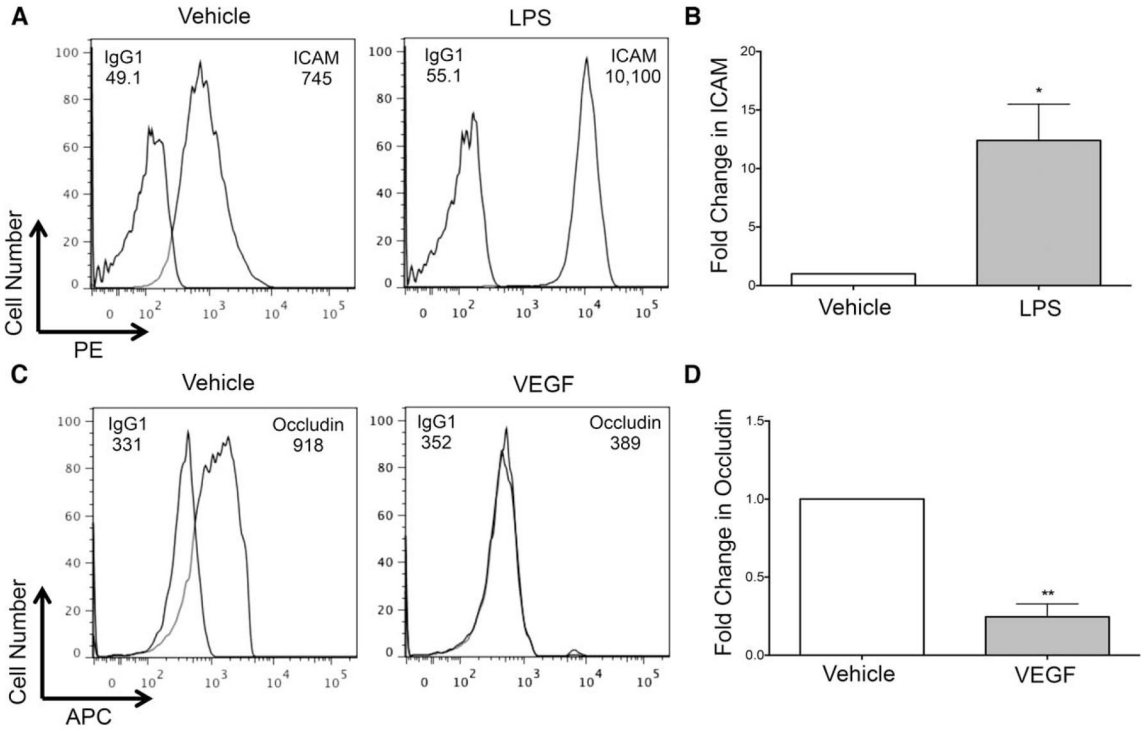

Figure 4.

BMVEC from BBB model are responsive to stimuli. BMVEC were recovered from the BBB using TrypLE following 24-h treatment with 10 ng/mL LPS or VEGF, or PBS vehicle control. Histograms from one representative experiment demonstrate the (A) PE signal for ICAM, (C) APC signal for occludin, or the appropriate isotype-matched control, and their respective MFI. After subtracting the contribution of the isotype control, the pooled fold change in (B) ICAM MFI following LPS treatment or (D) occludin MFI following VEGF treatment (filled bar) relative to vehicle (open bar, set to 1) from five or three independent experiments, respectively, was determined. Data are represented as mean ±standard error of the mean. Significance was determined by a two-tailed paired *t*-test. **P* <0.05. ***P* <0.01.

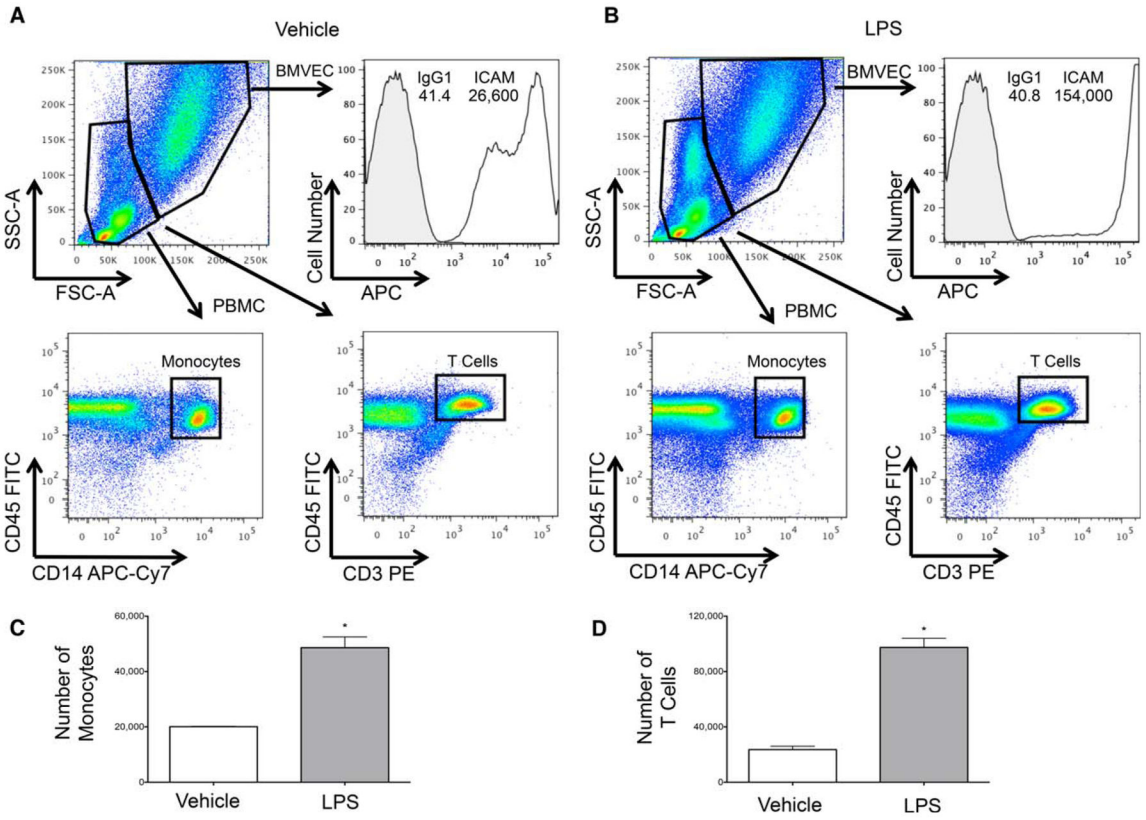

Figure 5.

Quantification of monocyte and T-cell adhesion to the BBB. PBMC were added to the BBB coculture model following pretreatment with (A) vehicle control or (B) 10 ng/mL LPS. Following 1 h of incubation and washing away nonadherent cells, TrypLE was used to collect the PBMC and the BMVEC from which they were interacting. SSC-A and FSC-A characteristics were used to create grates that discriminated between the PBMC and BMVEC. A histogram depicts BMVEC ICAM expression from one representative experiment. Rectangle gates were applied to the $CD45^{+}CD14^{+}$ and $CD45^{+}CD3^{+}$ PBMC populations and the number of cells within these gates enumerated. The number of (C) monocytes and (D) T cells that adhered to the BMVEC upon vehicle and LPS treatment in three separate experiments was determined. Data are represented as mean ±standard error of the mean. Significance was determined by a two-tailed paired *t*-test. ** $P < 0.01$. [Color figure can be viewed in the online issue, which is available at wileyonlinelibrary.com.]

Table 1

Compensation matrix for hardware compensation

FLUORESCENCE PARAMETER #1	FLUORESCENCE PARAMETER #2	PERCENT SPECTRAL OVERLAP
PE	FITC	18.05
APC	FITC	0
APC-Cy7	FITC	0
FITC	PE	1.25
APC	PE	0
APC-Cy7	PE	0
FITC	APC	5.09
PE	APC	3.70
APC-Cy7	APC	13.95
FITC	APC-Cy7	2.43
PE	APC-Cy7	1.58
APC	APC-Cy7	23.37

Table 2

Dissociation times and cell viabilities upon recovery of BMVEC from the BBB model with differing reagents (n =3; mean-±standard deviation is indicated)

REAGENT	DISSOCIATION TIME (MIN)	PERCENT VIABILITY
Trypsin	5.3 ±2.5	87.3 ±4.4
TrypLE	13.3 ±1.5	87.7 ±3.6
Accutase	30.0 ±15.0	85.6 ±0.7
Lidocaine	35.7 ±4.0	86.3 ±1.6
EDTA	41.0 ±3.6	85.9 ±2.0